Delayed Success in Termination of Three-Dimensional Reentry: Role of Surface Polarization

CHRISTIAN ZEMLIN, PH.D., SERGEY MIRONOV, PH.D., and ARKADY PERTSOV, PH.D.

From the Department of Pharmacology, SUNY Upstate Medical Center, Syracuse, New York, USA

Delayed Success and Surface Polarization. ***Introduction*: Defibrillation shocks slightly stronger than cardioversion threshold may defibrillate not immediately but after a transient period of postshock activity (delayed success). The effect of a defibrillation shock is that it polarizes the tissue, primarily at the surfaces; therefore, surface polarization may play an important role at near-threshold shock intensities.**

Methods and Results: **We numerically investigate the effect of a monophasic transmural electrical shock on a three-dimensional (3D) reentrant wave (scroll wave). For simplicity, we assume uniform polarization of the epicardial and endocardial surfaces. We demonstrate that the effect of surface polarization alone is sufficient to induce delayed termination of self-sustained activity (3–4 beats after the shock). In agreement with experimental observations, both successful and failed shocks cause prolongation of the action potentials on the depolarized side and shortening on the hyperpolarized side, while at the same time inducing a shift from a reentrant to a focal activation pattern. Our simulations suggest that the outcome of the shock is determined by its effect on the shape of the scroll wave's center of rotation (filament). We propose a simple rule to predict the postshock filament shape that allows us to make accurate predictions of success and failure of a termination attempt.**

Conclusion: **Surface polarization due to an electrical shock can terminate a reentrant scroll wave. This mechanism may explain the phenomenon of delayed success in defibrillation.** *(J Cardiovasc Electrophysiol, Vol. 14, pp. S257-S263, October 2003, Suppl.)*

delayed success, defibrillation, reentry, polarization

Introduction

Ventricular fibrillation (VF) is one of the leading causes of death. Although its mechanism remains incompletely understood, it is established that, during VF, one or more three-dimensional (3D) reentrant waves (scroll waves) are active in the heart. In defibrillation, these scroll waves are eliminated by application of an electrical shock. The success of defibrillation is not always immediate. Especially for shocks only slightly above the cardioversion threshold, defibrillation has been observed to succeed after a transient period of postshock activity (delayed success).[1-3] Here we study numerically the effect of surface polarization on the termination of 3D reentrant waves. We demonstrate that surface polarization may produce an effect reminiscent of delayed success, which may shed light onto the mechanism of this interesting phenomenon.

Multiple numerical and experimental studies demonstrate that electric stimuli produce highly nonuniform polarization of myocardial tissue.[4-8] The largest polarization has been shown to occur near the epicardial and endocardial surface, at the tissue-bath interface.[9-14] In particular, this polarization is significantly larger than the polarization produced by other nonuniformities inside the myocardial wall, such as curvature of myocardial fibers and discontinuous anisotropy. Despite its large magnitude, the surface polarization involves only a thin layer of myocardium (on the order of the electrotonic space constant $\lambda = 500\ \mu$m) and thus has never been considered a significant factor in defibrillation. As we demonstrate here, however, its importance may dramatically increase for near-threshold shocks where contributions of other polarization mechanisms become small. Our study suggests that although surface polarization cannot instantaneously terminate reentrant activity inside the tissue because of insufficient penetration depth, it may destabilize and terminate reentry via a different slow mechanism linked to 3D dynamics of the scroll wave filament.

It is well established that the stability of 3D reentrant activity and its lifespan critically depend on the shape of its filament, an organizing center about which the excitation wave rotates.[15-18] We demonstrate that surface polarization produced by the electrical shock can change the filament configuration in such a way that reentry becomes unstable and terminates after a few rotations, thus providing a mechanism for delayed success.

Methods

Tissue Model

We study basic mechanisms by which surface polarization can terminate scroll waves. To exclude complications due to the complex geometry of the heart, we consider a homogeneous block of myocardium. We use a monodomain FitzHugh-Nagumo-type model to account for electrophysiologic properties of the medium[19]:

$$\frac{\partial v}{\partial t} = \nabla \cdot (D\nabla v) - f(v,w)$$
$$\frac{\partial w}{\partial t} = g(v,w) \qquad (1)$$

This work was supported by a grant from the American Heart Association.

Address for correspondence: Christian Zemlin, Ph.D., Department of Pharmacology, SUNY Upstate Medical Center, 750 East Adams Street, Syracuse, NY 13210. Fax: 315-464-8014; E-mail: c.zemlin@biologie.hu-berlin.de

doi: 10.1046/j.1540.8167.90318.x

with $f(v,w) = v(v/d - 1.0)(1.0 - v/e) - w$, $d = 5$, $e = 100$, and $g(v,w) = c(v - bw)$, $b = 0.2425$, $D = 144.0$ as the diffusion constant, and c as the inverse time constant of the slow variable. The fast variable v in this model describes transmembrane voltage; the slow variable w describes inactivation and reactivation. We scale the transmembrane voltage by setting $V_m = (0.602v - 66.8)$ mV. To obtain a realistic, small excitable gap, the inverse time constant c of the slow variable is set to $c = 1.0$ for the excited state ($v > 0$) and $c = 2.0$ for the relaxed state ($v \leq 0$).

For numerical integration of Equation 1, we use the explicit Euler method with Neumann boundary conditions. The domain is a 3D orthogonal grid, and we choose a dimensionless time step of 0.001. The error in these computations, estimated using the difference between the numerically calculated velocities of plane wave propagation,[20] is <5%.

By assigning the dimensionless time unit a duration of 24 msec and grid constant a length of 340 μm, we get wave propagation characteristics similar to that in the real heart: action potential duration (APD) = 250 msec, propagation velocity = 50 cm/s, and spiral wave length = 7.2 cm.

The physical dimensions of our medium are 34 × 11.3 × 8.5 mm, typical of the porcine right ventricular wall preparation with a thickness of about 8 mm. We also include anisotropy. We assume a fiber orientation that is intramural and horizontal, i.e., along our y-axis, everywhere (see Fig. 2D). The anisotropy ratio (conduction velocity along fibers divided by conduction velocity across fibers) is set to 3:1.[21,22] To account for this anisotropy, we use three times as many grid points in the directions perpendicular to fiber orientation than suggested by the physical dimensions of our tissue block (we use 100 × 100 × 75 instead of 100 × 33 × 25 grid points), but we use an isotropic diffusion tensor.

Scroll Wave Initiation

We initiate a 3D plane wave moving from left to right on a square 100 × 100 × 75 grid. As the wavefront passes the middle of the medium, we induce a spiral wave via cross-field stimulation. We allow the spiral wave to stabilize for five rotations and wait an additional variable time until the scroll wave reaches the orientation we desire for the individual simulation. Then we immediately apply a shock. In some simulations, we wanted more control over the filament position at the moment of shock. In these cases, we initiated the spiral in a 200 × 200 × 75 block and selected a 100 × 100 × 75 region directly before the shock.

Shock Protocol

We model a transmural shock. Such a shock leads to polarization of inhomogeneities and, most importantly, of the preparation surfaces, according to experiments[12] and theoretical studies[9,13,23] using bidomain models.[24] In accordance with theoretical studies,[9] we introduce a transmembrane shock current I_{shock} of the form:

$$I_{shock}(x) = I_0 \frac{\sinh((x - x_m)/\lambda)}{\sinh(x_m/\lambda)}, \qquad (2)$$

where x is the position along the cross-section of the wall, x_m is the position of the midpoint of the wall, λ is the characteristic attenuation length[12,13] of the polarization, and I_0 is the shock current amplitude (assuming a specific membrane capacitance of 1 $\mu F/cm^2$). In our simulations, we used

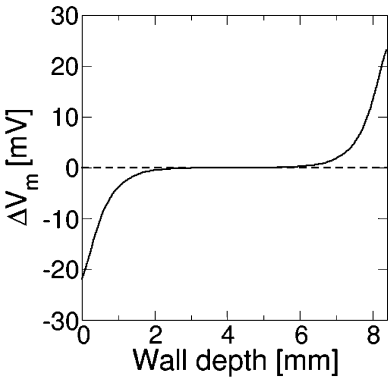

Figure 1. *Tissue polarization due to the shock. The shock was applied to quiescent medium. Change in transmembrane voltage across the wall 500 μsec into the shock is shown.*

$x_m = 4.25$ mm, $\lambda = 500$ μm, $I_0 = 3$ μA/cm^2, and a shock duration of 9.6 msec. The minimum shock amplitude necessary to initiate a propagating wave at this shock duration is 0.1 μA/cm^2. The effect of the specified shock on resting tissue is shown in Figure 1, where we plot the transmembrane voltage distribution across the ventricular wall 500 μsec into the shock.

Filament Detection

For visualization of the filament, we use a technique introduced by Biktashev et al.[18] We define the filament to consist of all points for which $v_{min} < v < v_{max}$ and $w_{min} < w < w_{max}$, where v_{min}, v_{max}, w_{min}, and w_{max} are threshold values that should be adjusted for good visibility of the filament in visualizations.

Results

Delayed Success

We discovered that surface polarization produced by an electrical shock alone can terminate sustained three-dimensional reentrant activity. Although surface polarization does not penetrate deeply into the tissue and thus cannot terminate reentry instantly, it is sufficient to destabilize sustained scroll waves, causing their termination after several rotation cycles ("delayed success"). Figure 2 shows an example of shock-initiated delayed termination of a stable transmural scroll wave. Panel A shows the simulated transmembrane voltage before, during, and after the shock, recorded from a point 50 μm below the depolarized surface. Prior to the shock, the scroll rotates with a period of $T = 210$ msec and $APD_{50} = 131$ msec. Note the significant prolongation of the action potential ($APD_{50} = 171$ msec) after the shock. The magnitude of the prolongation varies with the location of the recording site (not shown). Such prolongation is consistent with the experimental observations by Dillon et al.[25,26] and is a result of the external depolarizing current provided by the shock. The prolongation of the action potential does not have an immediate effect: periodic activity resumes at a slightly shorter period ($T = 204$ msec and an APD_{50} ranging from 126 to 148 msec) to generate four more action potentials. Only then does the periodic activity abruptly terminate.

Panels B and C show the opposite, hyperpolarized side of the myocardial wall. In contrast to panel A, the action

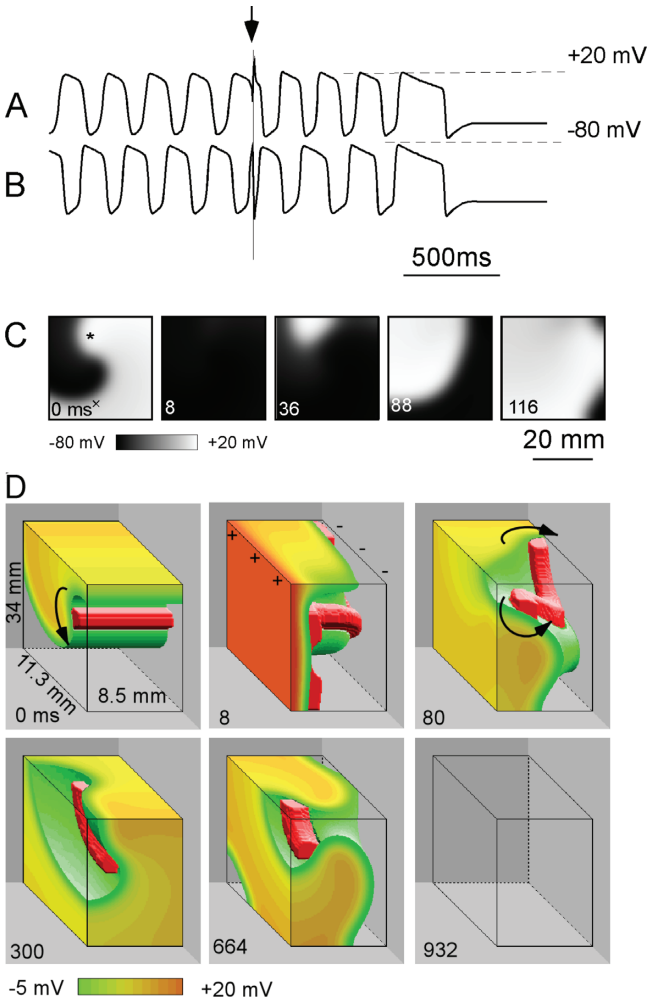

Figure 2. *Delayed success due to surface polarization. A: Transmembrane voltage recording from a point 50 μm below the depolarized side of the block. The arrow marks the moment at which the shock is applied. The location of the recording on the depolarized surface is marked by "×" in panel C; the location of the recording on the repolarized side is marked by "∗". B: Transmembrane voltage recording from a point 50 μm below the hyperpolarized side of the block. C: Activation of the surface hyperpolarized by the shock. Gray-scale levels code the transmembrane voltage, with black for relaxed tissue (≈ −80 mV) and white for excited tissue (≈ 20 mV). Numbers in the lower left-hand corner indicate time since the beginning of the shock (in milliseconds). D: Color-coded transmembrane voltage at the surface and the isosurface of the cutoff level (5 mV). The filament of the scroll wave is shown in red. Arrows indicate the direction of scroll wave propagation. The "−" and "+" signs indicate the polarity of the transmembrane shock current at the left and right surface, respectively. Numbers in the lower left-hand corner indicate time since the beginning of the shock (in milliseconds).*

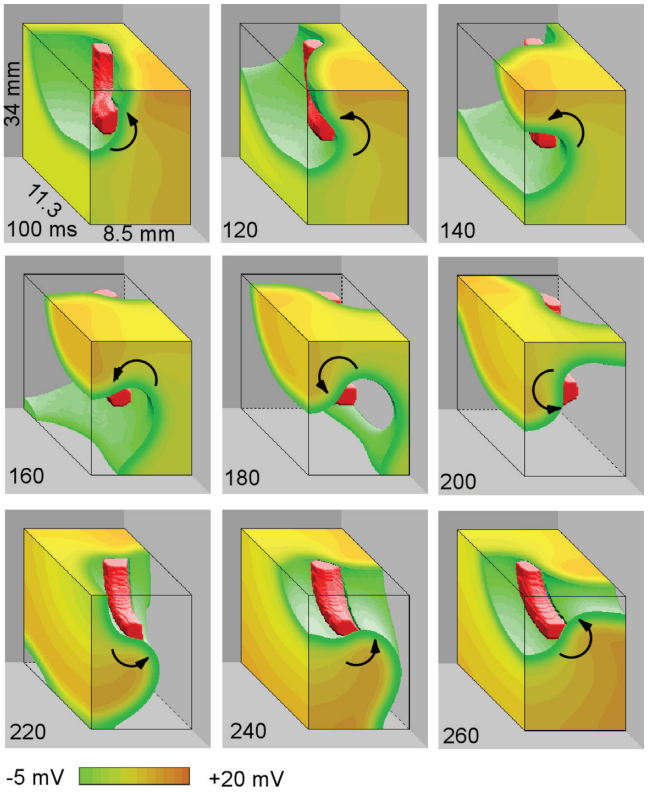

Figure 3. *One full rotation of the postshock wave around its L-shaped filament. See Figure 2 legend for details.*

potential is shortened ($APD_{50} = 22$ msec). A similar shortening of action potentials has been experimentally observed during defibrillation by Efimov et al.[8] Panel C shows sequential snapshots of the excitation wave prior to and after the shock. The shock hyperpolarizes all of the surface to a level below resting potential (8 msec). After some delay, the first postshock activation sets in (36 msec). It resembles the activation sequence of a point source, emanating from the upper left-hand corner and spreading over the surface (88, 116 msec).

Although surface manifestations of the shock presented here are important to illustrate the relevance of our simulations to the experiment, the key to understanding the mechanism of delayed success is to consider the shock-induced changes of the scroll wave filament, the organizing center of 3D reentry. We demonstrate that delayed success can be the result of detaching the filament from the endocardial and epicardial surfaces and reshaping it into an unstable L-shape. The first panel of Figure 2D (0 msec) shows in green the preshock scroll wave. The linear (stable) transmural filament is shown in red. The next panel shows how the shock polarizes the surfaces (8 msec). The polarization detaches the filament ends and shifts them to the upper and front surfaces of the tissue block, which is less affected by the shock (80 msec). This gives rise to an L-shaped filament (below we call filaments "L-shaped" when they connect adjacent sides of the tissue slab). The L-shaped filament shrinks continuously (300, 664 msec). Finally, the excitation wave fails to propagate through the narrow isthmus formed by the filament in the upper near edge of the tissue slab where the reentry terminates (932 msec).

Figure 3 shows in detail one rotation cycle of the L-shaped scroll wave 100 msec after its initiation by the shock. The upper three panels show the excitation wave squeezing through the isthmus. Note that it takes almost 80 msec (from 100 to 180 msec) for the wave to pass the isthmus. Passing the isthmus corresponds to slightly more than a quarter turn of the scroll wave, but 80 msec is much more than one quarter of the full rotation cycle (204 msec). The remaining three quarters of the turn are completed at a higher speed.

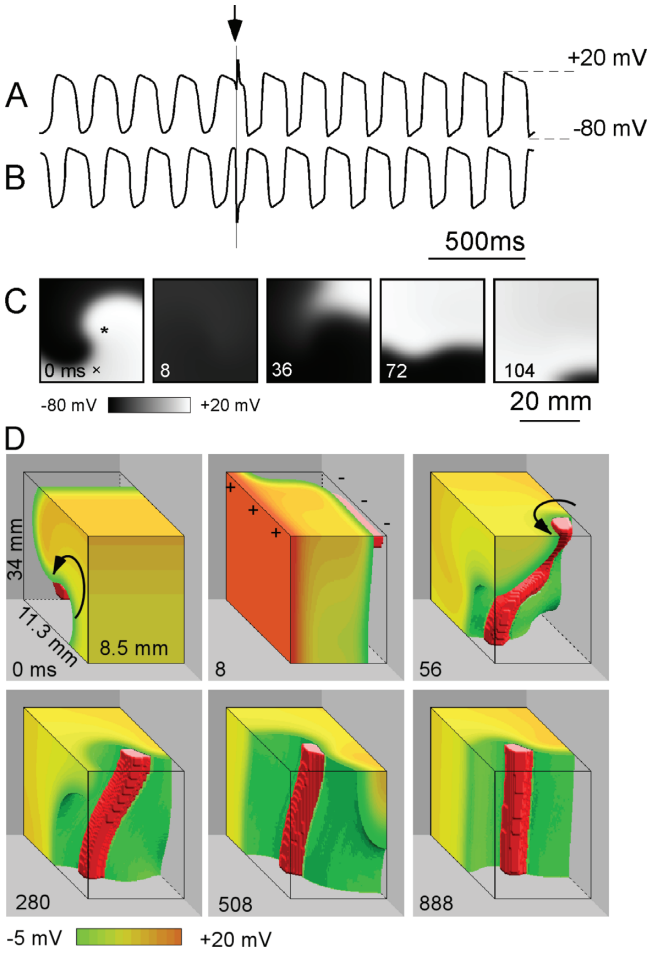

Figure 4. *Failed termination attempt. A: Action potential from a point close to depolarized side of the block. B: Action potential from a point close to hyperpolarized side of the block. C: Activation of the surface hyperpolarized by the shock. See Figure 2 legend for details. D: Color-coded transmembrane voltage at the surface and the isosurface of the cutoff level. See Figure 2 legend for details.*

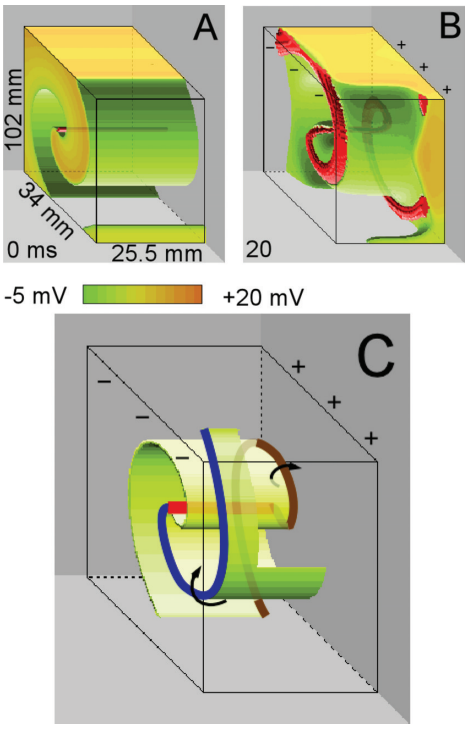

Figure 5. *Transformation of the filament due to surface polarization in a large medium. A: Scroll wave prior to the shock. B: After the shock, the filament has been detached from its original touching points because of the polarization of the surfaces. C: Schematic explanation of the postshock filament structure. A scroll wave directly after the application of a shock is shown. The "+" and the "−" signs mark the depolarized and the hyperpolarized surface, respectively. The red line marks the remainder of the preshock filament; the blue curve marks the new filament fragment at the hyperpolarized side, and the brown curve marks the new filament fragment at the depolarized side. Arrows indicate how excitation propagates around the postshock filament.*

The effect of delayed success in termination of reentry due to surface polarization is robust and can be observed in a wide range of shock durations and amplitudes (see later).

Termination Failure

The shock fails to terminate reentry if its timing is not right. Figures 4A and 4B show surface recordings from an unsuccessful termination attempt. The initial conditions are identical to those of the successful attempt, except for the timing of the shock.

Panel A shows a recording of the transmembrane potential from a point 50 μm below the depolarized surface. As in the successful case, the shock prolongs an action potential (from APD_{50} = 129 msec to APD_{50} = 155 msec), but the point is quickly reexcited as the reentrant activity resumes. However, in this case the periodic activity does not spontaneously terminate.

Panel B shows a recording from a point 50 μm below the hyperpolarized surface. As in the successful case, the shock shortens an action potential (from APD_{50} = 120 msec to APD_{50} = 40 msec) and afterward periodic activity resumes. Panel C shows snapshots of activity of the hyperpolarized

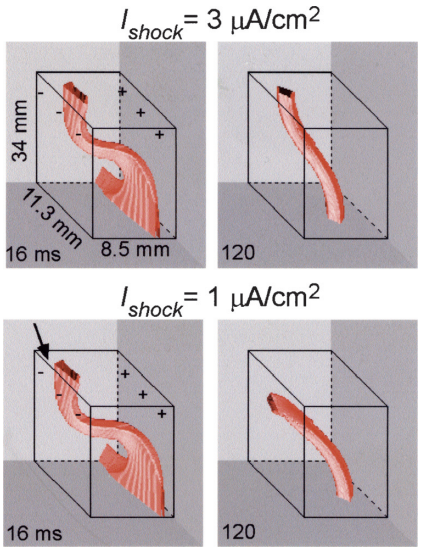

Figure 8. *Filament shapes after strong and weak shock. The upper two panels show the effect of a strong shock (3 μA/cm^2) on the filament shortly after the end of the shock (16 ms) and after 120 ms. Lower two panels show the corresponding snapshots for a weak shock (1 μA/cm^2), with identical preshock conditions. The arrow points to the small gap between the surface and the postshock filament in the case of a weak shock where reattachment takes place. The "+" and "−" signs mark the depolarized and the hyperpolarized surface, respectively.*

side of the tissue block. Similar to the successful termination case, the preshock scroll wave is almost completely wiped out on the surface by the shock (8 msec). With some delay, there is activation that resembles a point source (36, 72, 104 msec).

Interestingly, the direct effect of the shock is strikingly similar for both successful and unsuccessful termination attempts. So why does periodic activity terminate after a few rotations in one case and stabilize in the other? The answer lies in the shape of the postshock filament (Fig. 4D). Whereas successful shocks produce an L-shaped filament, which shrinks to nothing, failing shocks produce a filament configuration that converges to a stable I-shaped filament (we call a filament "I-shaped" if its ends terminate on opposing surfaces). In both cases, the preshock wave (0 msec) is detached from the polarized surfaces (8 msec). However, in the unsuccessful case, the ends of the newly formed filament are located on opposite sides (top and bottom) of the tissue slab (56 msec). In this case, the shrinking of the filament does not cause the collapse of the filament but instead produces a stable rectilinear I-shaped filament. The filament shrinks continuously (280 msec) until it becomes a straight line (508, 888 msec) and further shrinkage is impossible. Note that the final filament is orthogonal to the original filament.

Shape of the Postshock Filament

The shape of the postshock filament is determined by the orientation of the scroll wave at the moment of shock. To understand the formation of the postshock filament, it is helpful to consider a significantly bigger medium comprising one full turn of the scroll wave (Fig. 5A). In Figure 5B, we show the filament and wavefront shortly after application of a shock in a 102 × 34 × 25 mm medium. The postshock filament configuration is drastically different from the initial rectilinear shape shown in panel A. It consists of three distinct fragments: a central rectilinear fragment (the remainder of the original filament) and two newly formed, spiral-shaped fragments near the hyperpolarized and the depolarized surfaces, respectively.

These three fragments are shown in different colors in the schematic drawing in Figure 5C. On the depolarized side, a new spiral fragment of the filament (brown) is formed along the waveback, because the shock excites all the tissue in the vicinity of the surface except for the refractory tail of the rotating scroll wave. In contrast, on the hyperpolarized side of the tissue, a spiral fragment of the filament (blue) is created along the wavefront. On this side, the shock de-excites all the depolarized tissue except at the vicinity of the wavefront.

Predicting Termination Success

The postshock filament structure allows us to predict the outcome of a shock. Our simulations suggest that the shock usually is successful if, immediately after the shock, the ends of the filament are located on the adjacent surfaces of the tissue slab (Fig. 2D). In this case, the filament acquires an L-shape and eventually collapses. In contrast, if the ends of the filament appear on opposite surfaces of the slab, it shrinks to a stable rectilinear I-shaped filament without interrupting reentrant activity (Fig. 4D). Which of the two cases applies depends on the phase of the shock. This explains qualitatively the phase dependence of failure and success.

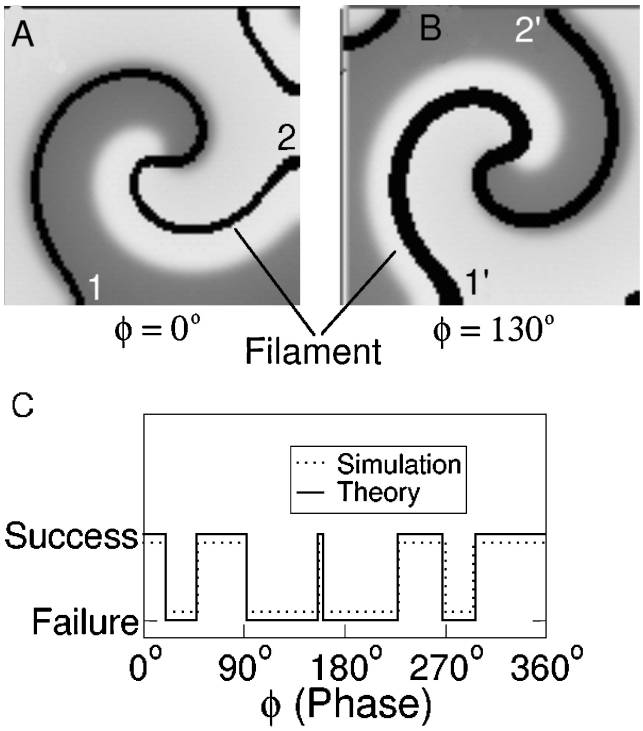

Figure 6. *Superposition of the wave prior to the shock and the postshock filament. Gray levels indicate transmembrane voltage; dark solid curves show the projections of the postshock filament. A: The scroll wave is oriented such that our proposed mechanism predicts an L-shaped filament and delayed success for termination. The filament ends are marked "1" and "2." B: The same scroll wave as shown in Figure 6A, at a later time. Now the scroll wave is oriented such that our mechanism predicts an I-shaped filament and failure of termination. The filament ends are marked "1′ " and "2′." C: Termination success depends on wave phase at the moment of shock. We apply an electrical shock to scroll waves of different phases and test whether the mechanism explained in Figure 5 correctly predicts termination success as observed in simulations. Prediction and real outcome of termination attempts are shown in the graph as functions with two possible values (success/failure). The trace of the simulation results has been slightly shifted for better visibility.*

To test this method of prediction, we superimposed the projections of the preshock wave and the postshock filament (Fig. 6). Figure 6A and 6B show the epicardial projection of postshock filament configurations for successful and unsuccessful shocks, respectively. In the first case, one can see that the ends of the filament are at the bottom and right boundaries (marked by "1" and "2"). As expected, the filament collapses. In the second case, the ends are located on opposite sides (top and bottom, marked by "1′" and "2′"). In this case, the filament becomes rectilinear and reentry does not terminate.

Importantly, prediction of the delayed success and failure can be obtained directly from the shape of the wave at the moment of the shock. As can be seen from panels A and B, the epicardial projection of the spiral fragments of the postshock filament follow the wavefront and waveback of the preshock scroll wave. However, there is a mismatch between the filament position and the position of the wavefront and tail. To make an accurate prediction of the post-shock filament configuration and thus the outcome of the shock, one should take into account this mismatch.

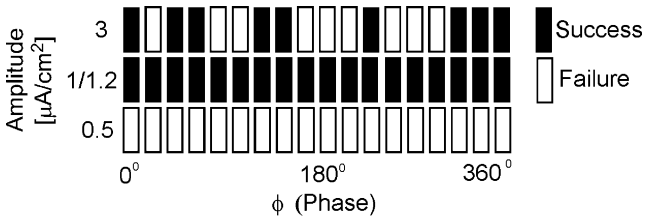

Figure 7. *Termination success/failure as a function of shock phase and amplitude. In the middle row, the amplitude used is 1 μA/cm^2, except for the phases 320 and 0°, where it is 1.2 μA/cm^2, because for these phases, the cardioversion threshold was higher. Medium size was 34 × 11.3 × 8.5 mm.*

Here we derive an empirical rule that improves significantly the prediction of postshock filament shape. To quantify the lag of the filament behind the wave, we introduce the *phase* of a preshock scroll wave, an angle describing its orientation, in the following way. We choose an arbitrary reference state of the scroll wave to be phase 0° (Fig. 6A). The state precisely one full rotation later is assigned phase 360°. All intermediate states are assigned phases such that the increase of phase with time is constant. In these terms, the lag of the filament behind the preshock wave is 46° for the front and 12° for the back.

Figure 6C compares the theoretical prediction based on the corrected phase-shifted configuration of the preshock wave (solid line) with the actual simulation results (dashed line). To make this comparison, we applied shocks to scroll waves of different phases ranging from 0° to 360°. We predicted the postshock filament shape by phase shifting the wavefront by 46° and the waveback by 12°. The outcome of the shock was predicted based on the position of the filament ends as described earlier and then compared with the actual outcome. Figure 6C shows excellent agreement between predicted and actual outcomes.

Factors Affecting Termination Time

In the case of successful termination, the time the scroll wave takes to disappear strongly depends on the size of the medium (shorter time for smaller media) and the position of the filament (shorter time for filament close to the boundary). This should be expected because the filament contracts faster where it is more curved.[17] Larger media typically lead to a longer postshock filament. After initial regions of high curvature flatten out, the remaining long filament takes a long time to disappear. Similarly, centered scroll waves produce longer postshock filaments that take longer to disappear. For preshock filaments close to the border of the medium, the postshock filament can become arbitrarily short. In our medium, the duration of delayed success varied from one rotation for filaments close to the boundary to over 30 rotations for a centered filament in a large medium.

Effect of Stimulus Amplitude

A shock that is not sufficiently strong to change the topology of the preshock filament fails to terminate the scroll wave. We call the minimal shock amplitude necessary for terminating a stable scroll wave the *cardioversion threshold*. In our simulations, the cardioversion threshold was 7 to 8 times the excitation threshold for field stimulation. Figure 7 illustrates the effects of shocks of three different amplitudes. For low amplitudes (1 μA/cm^2), the shocks fail because the original scroll wave persists. For larger shocks of 3 μA/cm^2, termination success depends on phase, as discussed earlier. Similar to Figure 6C, we observe four phase intervals in which the shocks are successful and four phase intervals in which the shocks fail.

We discovered, however, that shocks of intermediate amplitude ($\approx$1 μA/cm^2) always terminate reentry, independently of phase (Fig. 7). The explanation for this is provided in Figure 8, which compares the effect of a strong and a weak shock. Both shocks initially detach the filament from the depolarized and the hyperpolarized side, but in the case of the weak shock, the filament is formed significantly closer to the surface (see arrow in bottom left panel). As a result, one of its ends quickly reattaches to the hyperpolarized side. Reattachment occurs independently on timing of the shock and always produces an L-shaped filament.

Discussion

We showed that surface polarization induced by electric shocks destabilizes reentrant waves. The destabilized waves may collapse within a few rotations, consistent with experimental observations of delayed success in defibrillation.

Our model reproduces the most important shock effects as they are commonly described. We see action potential prolongation at the depolarized side[12,25-28] and action potential shortening on the repolarized side.[8] The first postshock surface activation sequence resembled that of focal activation, as observed by Chattipakorn et al.[3,29,30]

Many defibrillation studies have shown that successful and unsuccessful defibrillation shocks are initially hard to distinguish.[3,30] This is true in our model as well, and the model provides an explanation. The postshock filament shape determines whether the shock will ultimately terminate reentrant activity. Similar preshock orientations lead to similar postshock filaments. There are, however, critical shock strengths and wave orientations at which the topology of the postshock filament (L-shaped vs I-shaped) changes. Close to these critical orientations, a small difference in orientation or shock strength can lead to a radically different outcome.

In the case of successful termination, the lifetime of the scroll wave depends on the position of the filament in the medium at the moment of shock, with filaments close to the boundary having the shortest lifetime.

The effectiveness of a shock also depends on the properties of the tissue-bath interface. Specifically, the strength of the induced surface polarization depends on the conductivity of the surrounding bath.[31,32] This implies that the detachment of a filament could be suppressed by an insulating surface or a surrounding medium of decreased conductivity.

Besides transmural scroll waves, intramural scroll waves are believed to play an important role in cardiac arrhythmias.[33] However, the mechanism described is not likely to terminate intramural scroll waves because intramural filaments typically are too far from the surface to be removed by surface polarization. In addition, for transmural scrolls, surface polarization may induce new wavebreaks that develop into additional intramural scroll waves.

On the other hand, the mechanism we outline here may be applicable not only to transmural scroll waves. As shown by Fast et al.,[11] electrical shocks induce significant polarization

at clefts in the tissue. If a filament is anchored to such a cleft, the polarization of the cleft surfaces can detach the filament just like surface polarization can detach the filament from epicardial or endocardial surface.

Study Limitations

This study considers a basic mechanism of reentry termination, and its application to the heart is limited in several ways. We modeled a block of tissue, i.e., a much simpler geometry than the whole heart. In particular, the real heart does not have bounding surfaces beyond epicardium and endocardium, whereas in our block model, the interaction of the filament with the other faces of the block is important. The shape of the postshock filament shape likely will depend on heart wall curvature and tissue structure and should be further investigated.

In addition, we are looking at a single scroll wave, whereas there may be several scroll waves interacting in a complex way during ventricular fibrillation in the whole heart. Our model of electrophysiology reproduces only the basic wave characteristics (APD, conduction velocity, approximate AP shape).

The mechanism of scroll wave elimination we propose in this article assumes that filaments contract. That is the case in the discussed medium and in other media as well.[15,16] Although there is already significant theoretical understanding of filament dynamics,[17,18] it is not yet known whether filaments also contract in detailed ionic models or in real heart tissue.

Conclusion

Surface polarization due to an electrical shock can terminate a reentrant scroll wave by detaching its filament from the epicardial and endocardial surfaces. Termination does not occur instantaneously, but after several reentrant cycles. This mechanism may explain the phenomenon of delayed success in defibrillation.

Acknowledgments: The authors thank Dr. Marcel Wellner and Amy Hellinger for careful reading of the manuscript.

References

1. Chen PS, Shibata N, Dixon EG, Wolf PD, Danieley ND, Sweeney MB, Smith WM, Ideker RE: Activation during ventricular defibrillation in open-chest dogs. Evidence of complete cessation and regeneration of ventricular fibrillation after unsuccessful shocks. J Clin Invest 1986;77:810-823.
2. Walcott GP, Knisley SB, Zhou X, Newton JC, Ideker RE: On the mechanism of ventricular defibrillation. Pacing Clin Electrophysiol 1997;20:422-431.
3. Chattipakorn N, Fotuhi PC, Ideker RE: Prediction of defibrillation outcome by epicardial activation patterns following shocks near the defibrillation threshold. J Cardiovasc Electrophysiol 2000;11:1014-1021.
4. Knisley SB, Hill BC, Ideker RE: Virtual electrode effects in myocardial fibers. Biophys J 1994;66:719-728.
5. Roth BJ: A mathematical model of make and break electrical stimulation of cardiac tissue by a unipolar anode or cathode. IEEE Trans Biomed Eng 1995;42:1174-1184.
6. Wikswo JP, Lin SF, Abbas RA: Virtual electrodes in cardiac tissue: A common mechanism for anodal and cathodal stimulation. Biophys J 1995;69:2195-2210.
7. Trayanova N, Skouibine K, Aguel F: The role of cardiac tissue structure in defibrillation. Chaos 1998;8:221-233.
8. Efimov IR, Gray RA, Roth BJ: Virtual electrodes and deexcitation: New insights into fibrillation induction and defibrillation. J Cardiovasc Electrophysiol 2000;11:339-353.
9. Plonsey R, Barr RC, Witkowski FX: One-dimensional model of cardiac defibrillation. Med Biol Eng Comput 1991;29:465-469.
10. Krassowska W, Pilkington TC, Ideker RE: Periodic conductivity as a mechanism for cardiac stimulation and defibrillation. IEEE Trans Biomed Eng 1987;34:555-560.
11. Fast VG, Rohr S, Gillis AM, Kleber AG: Activation of cardiac tissue by extracellular electrical shocks: Formation of '"secondary sources" at intercellular clefts in monolayers of cultured myocytes. Circ Res 1998;82:375-385.
12. Fast VG, Sharifov OF, Cheek ER, Newton JC, Ideker RE: Intramural virtual electrodes during defibrillation shocks in left ventricular wall assessed by optical mapping of membrane potential. Circulation 2002;106:1007-1014.
13. Hooks DA, Tomlinson KA, Marsden SG, LeGrice IJ, Smaill BH, Pullan AJ, Hunter PJ: Cardiac microstructure: implications for electrical propagation and defibrillation in the heart. Circ Res 2002;91:331-338.
14. Eason J, Trayanova N: Phase singularities and termination of spiral wave reentry. J Cardiovasc Electrophysiol 2002;13:672-679.
15. Panfilov AV, Rudenko AN, Krinsky V: Scroll rings in three-dimensional active medium with two component diffusion. Biofizika 1987;31:850-854.
16. Keener JP, Tyson JJ: The motion of untwisted untorted scroll waves in Belousov-Zhabotinsky reagent. Science 1988;239:1284-1286.
17. Keener JP: The dynamics of three-dimensional scroll waves in excitable media. Physica D 1988;31:269-276.
18. Biktashev VN, Holden AV, Zhang H: Tension of organizing filaments of scroll waves. Phil Trans R Soc Lond A 1994;347:611-630.
19. FitzHugh R: Impulses and physiological states in theoretical models of nerve membrane. Biophys J 1961;1:445-465.
20. Khramov R: Circulation of a pulse in an excitable medium. [in Russian] Biofizika 1978;23:871-876.
21. Draper M: A comparison of the conduction velocity in cardiac tissue of various mammals. QJ Exp Physiol 1959;44:91-109.
22. Kadish A, Shinnar M, Moore EN, Levine JH, Balke CW, Spear JF: Interaction of fiber orientation and direction of impulse propagation with anatomic barriers in anisotropic canine myocardium. Circulation 1988;78:1478-1494.
23. Plonsey R, Barr RC: Effect of microscopic and macroscopic discontinuities on the response of cardiac tissue to defibrillating (stimulating) currents. Med Biol Eng Comput 1986;24:130-136.
24. Henriquez CS: Simulating the electrical behavior of cardiac tissue using the bidomain model. Crit Rev Biomed Eng 1993;21:1-77.
25. Dillon SM, Mehra R: Prolongation of ventricular refractoriness by defibrillation shocks may be due to additional depolarization of the action potential. J Cardiovasc Electrophysiol 1992;3:442-456.
26. Dillon SM, Kwaku KF: Progressive depolarization: a unified hypothesis for defibrillation and fibrillation induction by shocks. J Cardiovasc Electrophysiol 1998;9:529-552.
27. Efimov IR, Aguel F, Cheng Y, Wollenzier B, Trayanova N: Virtual electrode polarization in the far field: Implications for external defibrillation. Am J Physiol Heart Circ Physiol 2000;279:H1055-H1070.
28. Cheng Y, Mowrey KA, Wagoner DRV, Tchou PJ, Efimov IR: Virtual electrode-induced reexcitation. Circ Res 1999;85:1056-1066.
29. Chattipakorn N, Banville I, Gray RA, Ideker RE: Mechanism of ventricular defibrillation for near-defibrillation threshold shocks: A whole-heart optical mapping study in swine. Circulation 2001;104:1313-1319.
30. Chattipakorn N, Fotuhi PC, Chattipakorn SC, Ideker RE: Three-dimensional mapping of earliest activation after near-threshold ventricular defibrillation shocks. J Cardiovasc Electrophysiol 2003;14:65-69.
31. Latimer DC, Roth BJ: Effect of a bath on the epicardial transmembrane potential during internal defibrillation shocks. IEEE Trans Biomed Eng 1999;46:612-614.
32. Entcheva E, Eason J, Efimov IR, Cheng Y, Malkin R, Claydon F: Virtual electrode effects in transvenous defibrillation-modulation by structure and interface: Evidence from bidomain simulations and optical mapping. J Cardiovasc Electrophysiol 1998;9:949-961.
33. Berenfeld O, Pertsov AM: Dynamics of intramural scroll waves in a 3-dimensional continuous myocardium with rotational anisotropy. J Theor Biol 1999;199:383-394.